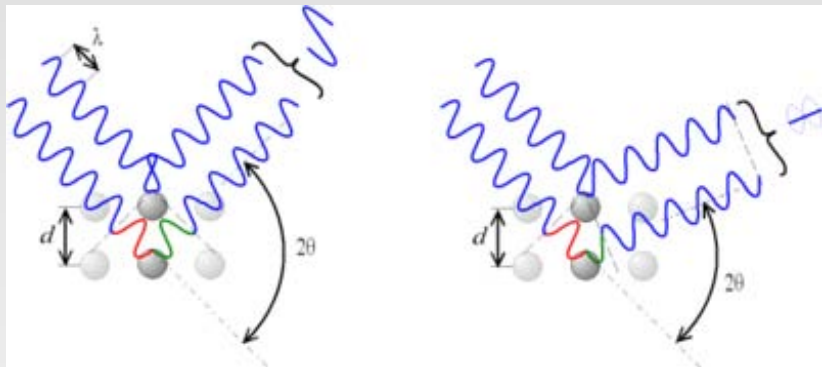


Crystallography & Cryo-electron microscopy

Methods in Molecular Biophysics, Spring 2010

Sample preparation
Symmetries and diffraction
Single-particle reconstruction
Image manipulation

Basic idea of diffraction: Bragg's Law



$$n\lambda = 2d \sin \theta$$

Identity operation

Plane Point Group

1

A single left-handed object. The corresponding point group with a right foot may also exist. The pair are said to be enantiomorphous. The single element of the point group is the identity operation.

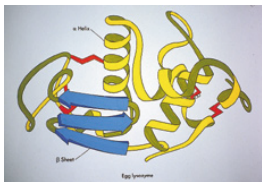
Symmetry operations:

$$E: x, y \rightarrow x, y$$

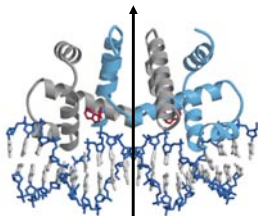
Multiplication table:

E

Order of group: 1



Two-fold symmetry operation



Two left feet related by a 2-fold rotation axis.

Symmetry operations:

$$E: x, y \rightarrow x, y$$

$$2: x, y \rightarrow -x, -y$$

Multiplication table:

$$E \ 2$$

$$2 \ E$$

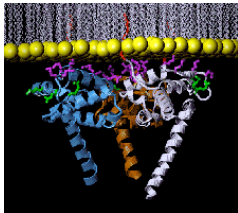
Order of group: 2

Plane Point Group

2



Three-fold symmetry operation



Plane Point Group

3 Three left feet, related by a 3-fold rotation axis. That the multiplication table for this group is symmetric, as it is for many others, is a consequence of the commutative property of the group. The product of any two symmetry operations may be taken in either order to obtain the same result.

Symmetry operations:

$$E: x, y \rightarrow x, y$$

$$3: x, y \rightarrow -\frac{1}{2}x - \frac{\sqrt{3}}{2}y, +\frac{\sqrt{3}}{2}x - \frac{1}{2}y$$

$$3^2: x, y \rightarrow -\frac{1}{2}x + \frac{\sqrt{3}}{2}y, -\frac{\sqrt{3}}{2}x - \frac{1}{2}y$$

Multiplication table:

$$E \ 3 \ 3^2$$

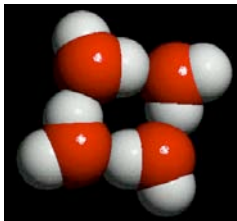
$$3 \ 3^2 \ E$$

$$3^2 \ E \ 3$$

Order of group: 3



Four-fold symmetry operation



Point Group **4** Four left feet, related by a 4-fold rotation axis. The operation 4^2 is equivalent to 2.

4

Symmetry operations:

$$E: x, y \rightarrow x, y$$

$$4: x, y \rightarrow -y, x$$

$$4^2: x, y \rightarrow -x, -y$$

$$4^3: x, y \rightarrow y, -x$$

Multiplication table:

$$E \quad 4 \quad 4^2 \quad 4^3$$

$$4 \quad 4^3 \quad E$$

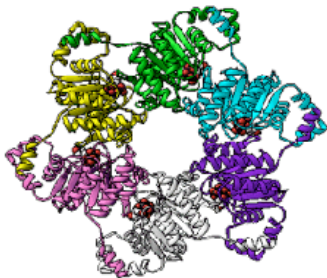
$$4^2 \quad 4^2 \quad E \quad 4$$

$$4^3 \quad E \quad 4 \quad 4^2$$

Order of group: 4



Six-fold symmetry operation



Plane Point Group: Six left feet, related by a 6-fold rotation axis.

6 Symmetry operations: E 6 6^2 6^3 6^4 6^5

The student should now be able to write the exact expressions for the coordinate transformations associated with each symmetry element. Note that

$$6^2 = 3$$

$$6^4 = 3^2$$

$$6^3 = 2$$

so that we could and often do write the symmetry elements as

$$E \ 6 \ 3 \ 2 \ 3^2 \ 6^5$$

Multiplication table: $E \ 6 \ 6^2 \ 6^3 \ 6^4 \ 6^5$

$$6 \ 6^2 \ 6^3 \ 6^4 \ 6^5 \ E$$

$$6^2 \ 6^3 \ 6^4 \ 6^5 \ E \ 6$$

$$6^3 \ 6^4 \ 6^5 \ E \ 6 \ 6^2$$

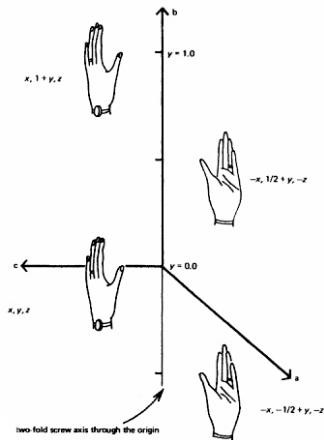
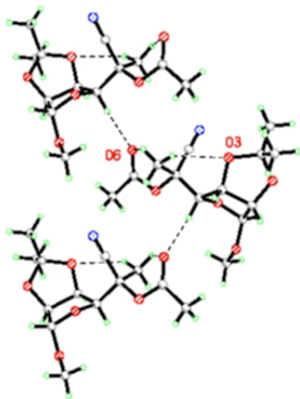
$$6^4 \ 6^5 \ E \ 6 \ 6^2 \ 6^3$$

$$6^5 \ E \ 6 \ 6^2 \ 6^3 \ 6^4$$

Order of group: 6



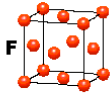
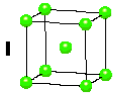
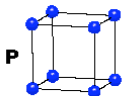
Screw axis = Rotational + Translational symmetry



This leads to repertoire of unit cells:

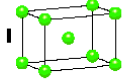
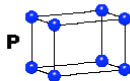
CUBIC

$$a = b = c$$
$$\alpha = \beta = \gamma = 90^\circ$$



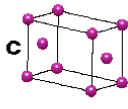
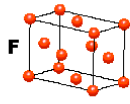
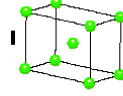
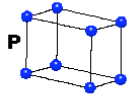
TETRAGONAL

$$a = b \neq c$$
$$\alpha = \beta = \gamma = 90^\circ$$



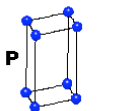
ORTHORHOMBIC

$$a \neq b \neq c$$
$$\alpha = \beta = \gamma = 90^\circ$$



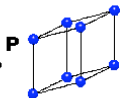
HEXAGONAL

$$a = b \neq c$$
$$\alpha = \beta = 90^\circ$$
$$\gamma = 120^\circ$$



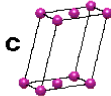
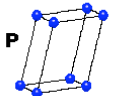
TRIGONAL

$$a = b = c$$
$$\alpha = \beta = \gamma \neq 90^\circ$$



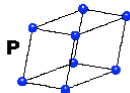
MONOCLINIC

$$a \neq b \neq c$$
$$\alpha = \gamma = 90^\circ$$
$$\beta \neq 120^\circ$$



TRICLINIC

$$a \neq b \neq c$$
$$\alpha \neq \beta \neq \gamma \neq 90^\circ$$



4 Types of Unit Cell

P = Primitive

I = Body-Centred

F = Face-Centred

C = Side-Centred

+

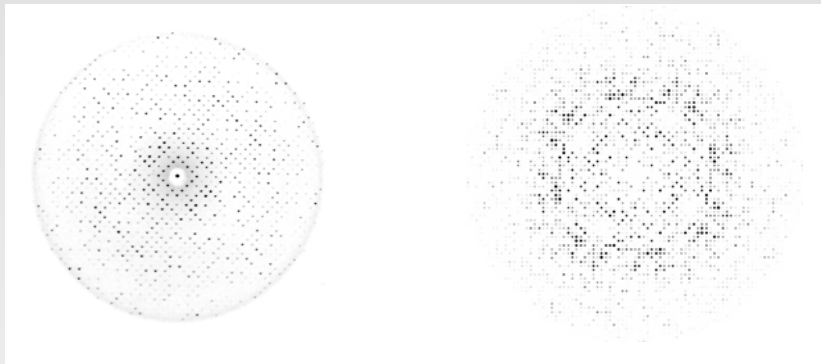
7 Crystal Classes

→ 14 Bravais Lattices

Protein spots from a protein crystal



trp repressor, two different crystal forms



Example of a reflection file

<u>H</u>	<u>K</u>	<u>L</u>	<u>intensity</u>	<u>error</u>
0	0	12	6714.3	347.2
0	0	18	-8.9	16.3
0	0	24	979.5	62.4
0	0	30	4136.4	272.5
1	0	3	3035.4	70.2
1	0	4	0.0	0.7
1	0	5	0.1	0.6
1	0	6	838.4	20.4
1	0	7	14903.0	535.6
1	0	8	2759.4	64.7
1	0	9	1403.5	31.0
1	0	10	109.4	5.6
1	0	11	31739.5	1611.5
1	0	12	231.9	7.6
1	0	13	5433.0	94.3
1	0	14	12392.7	211.4
1	0	15	3470.8	53.1
1	0	16	37.0	5.1
1	0	17	602.4	19.7
1	0	18	154.4	6.7
			...etc.	

Electron density calculation

$$\rho(x,y,z) = 1/v \sum_{hkl} \mathbf{F}_{hkl} e^{-2\pi i(hx + ky + lz)}$$

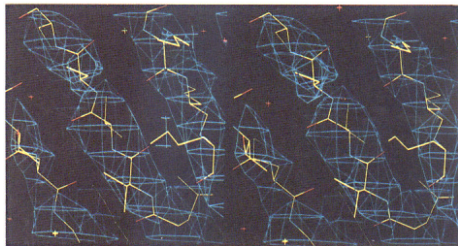
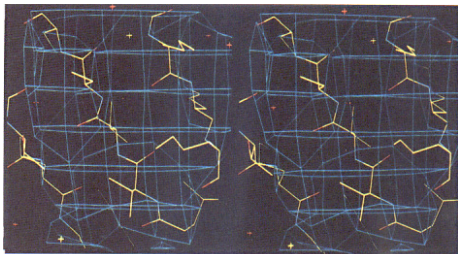
Reflection indices
of experimental
measurements

$$\mathbf{F}_{hkl} = |F_{hkl}| e^{2\pi i \phi_{hkl}}$$

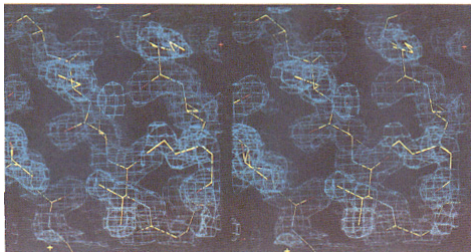
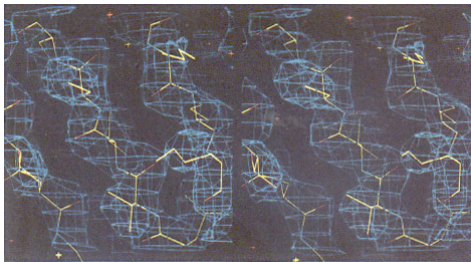
Amplitude:
from experimental
measurements

Phase:
must be estimated

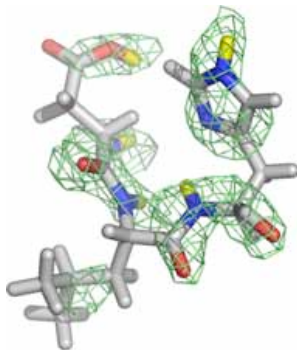
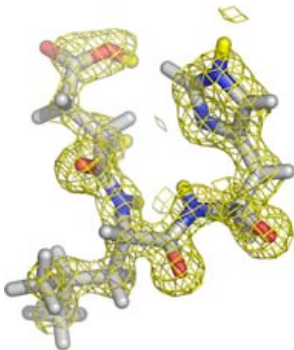
Protein maps at low resolution



Protein maps at higher resolution:

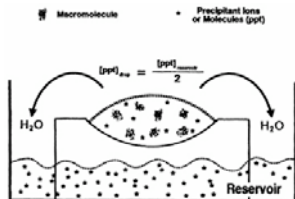
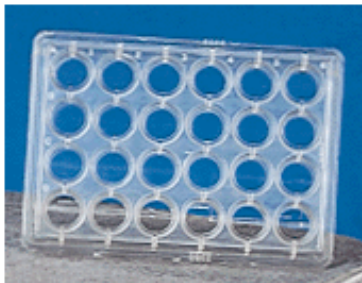


X-ray vs. neutron crystallography

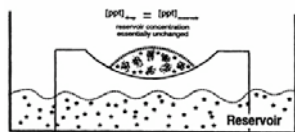


- H/D atoms are invisible to X-rays

Protein crystals are most often grown from vapor diffusion

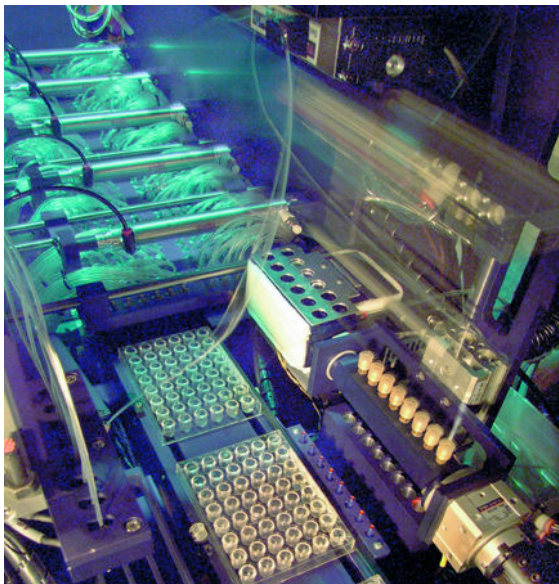


(A) Equilibration proceeds through vapor phase

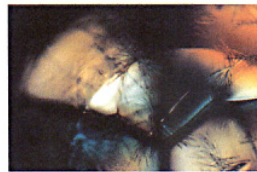
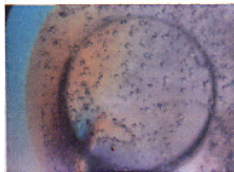
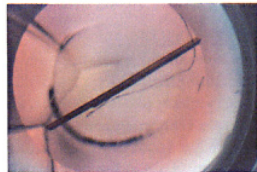
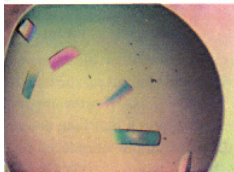
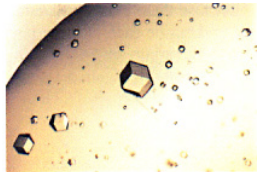


(B) Drop volume decreases, increasing concentration of both precipitant and protein

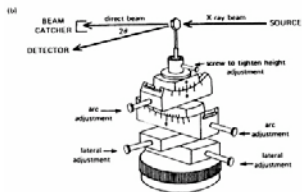
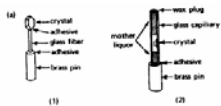
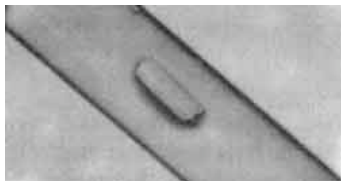
Robots increasing do the work



Some examples of protein crystals



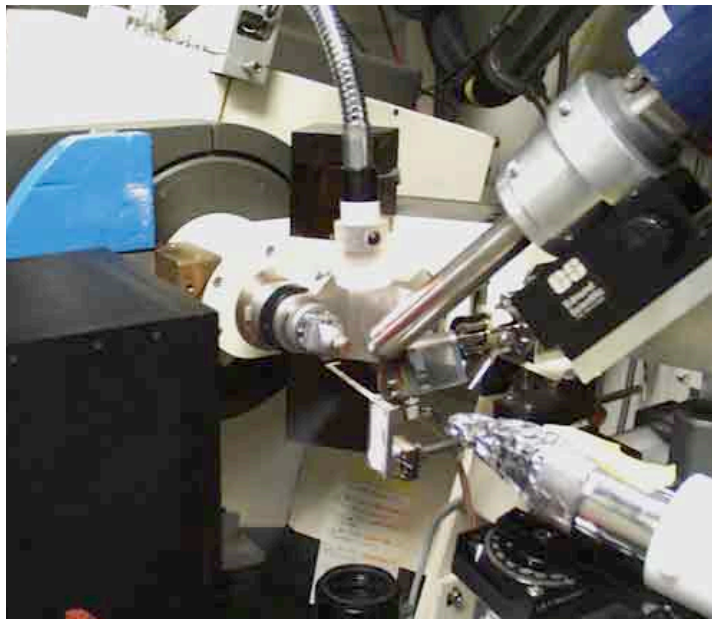
Mounting crystals



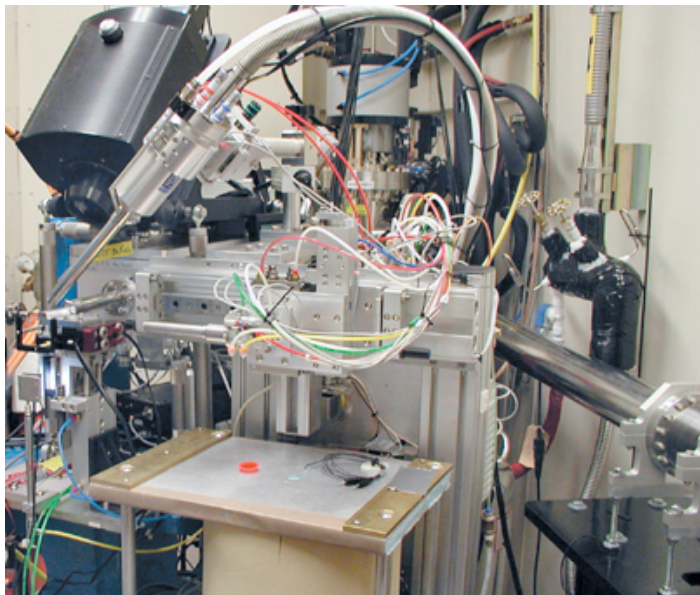
Laboratory data collection



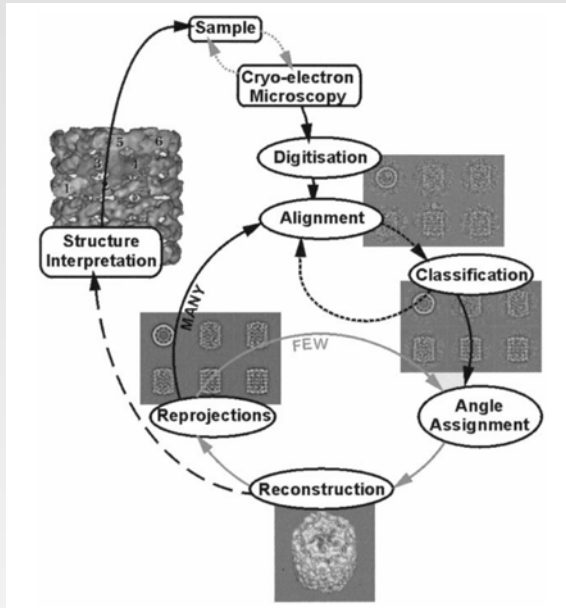
Details of a beam-line setup



Synchrotron crystal mounting robot

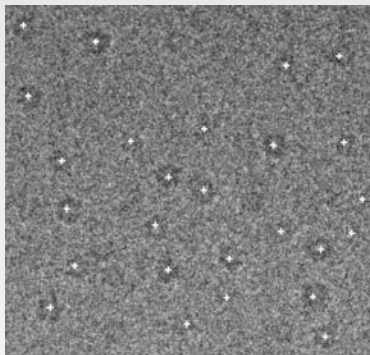
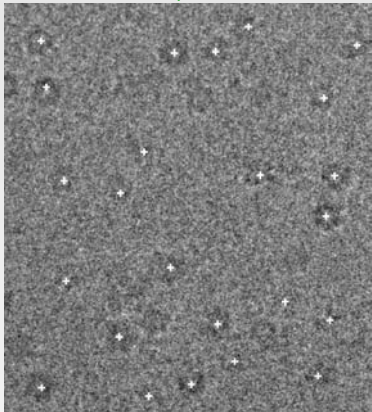


Overview of cryo-EM processing

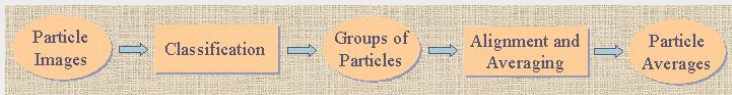
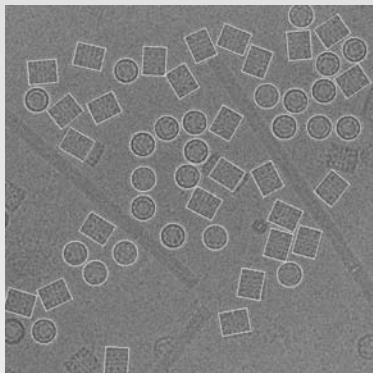
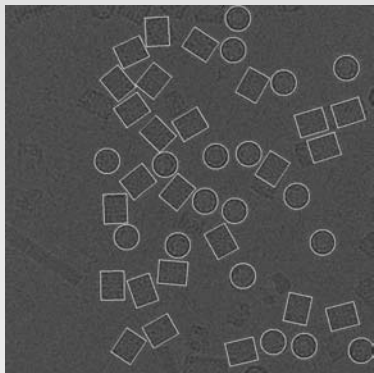


Particle picking

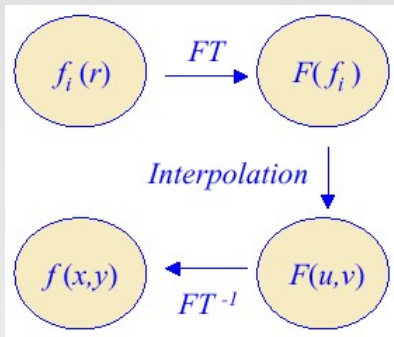
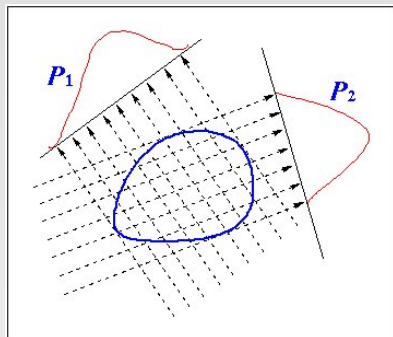
Particle detection is the first thing to do in the single particle reconstruction as soon as the Cryo-EM images are digitized and/or CTF-corrected. The goal of this step is to locate all particles. Since achieving high-resolution reconstruction often requires over hundreds of thousands of particles, it is important to design a fast and automatic algorithm for particle detection. We have developed two methods for this task. One is based on data clustering and the other is based on Voronoi diagram and distance transform. See <http://cvcweb.ices.utexas.edu/cvc/projects/angstrom/bm/index.php>



Automated particle picking



Projecting the image



The CT/MRI reconstruction is based on a theorem called Fourier Slice Theorem, which relates the Fourier transform of any projection of the original structure to the Fourier transform of the original structure. Fig.2(a) shows an example of a 2D structure reconstruction from its 1D projections. With enough number of projections, we can compute their Fourier transforms, each of which is "embedded" in the Fourier space and then an interpolation technique is used to "reconstruct" the Fourier transform of the original structure $f(x, y)$ in the entire Fourier space. After we obtain $F(u, v)$, the inverse Fourier transform of $F(u, v)$ gives the original structure $f(x, y)$. Fig.2 (b) illustrates the overall pipeline of reconstruction. It is straightforward to extend this procedure into 3D structure reconstruction.

More on projections

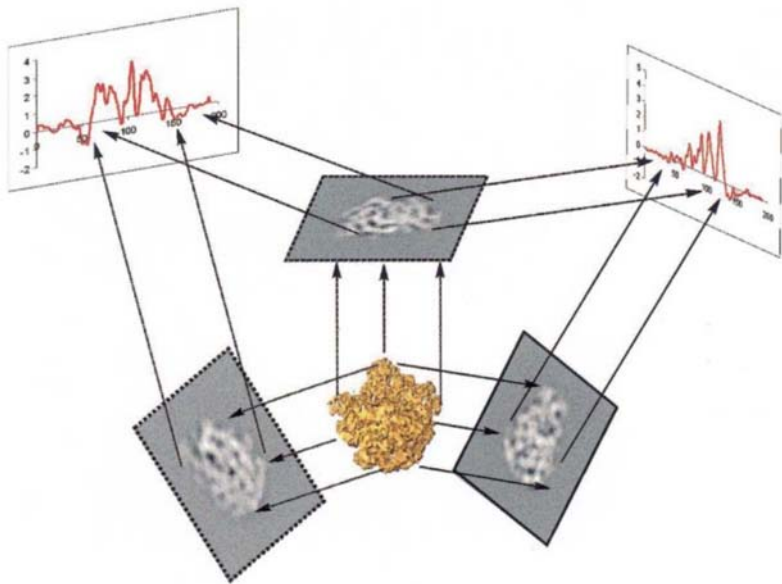


Image enhancement

The images obtained from the cryo-electron microscopy are usually very noisy and have very low contrast. It is necessary to smooth the noise as well as enhance the contrast. This also happens right after the 3D electron density maps are reconstructed. The following pictures show an example of our approaches on the reconstructed electron density map of Rice Dwarf Virus (RDV). The Cryo-EM images or the reconstructed maps may also be improved by Contrast Transfer Function (CTF) correction.

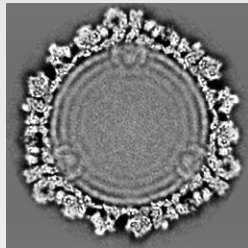
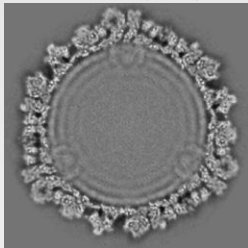
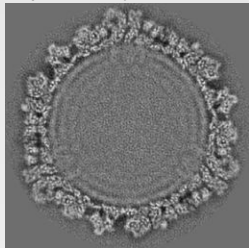
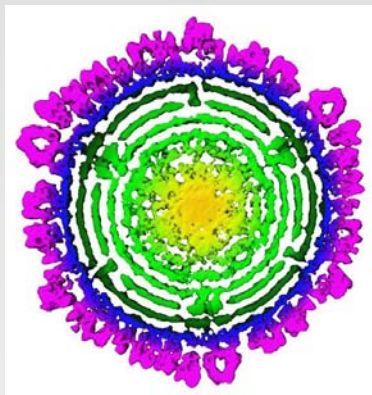
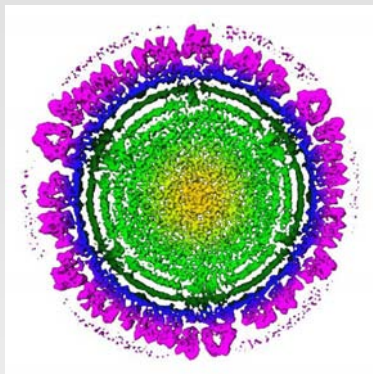


Image enhancement



Moving towards atomic resolution

Although atomic details are not detectable in reconstructed 3D cryo-EM maps, given their low feature resolution, it is sometimes feasible to locate secondary structures (alpha helices and beta sheets). An approach for detecting alpha helices in 3D maps is where the alpha helix is modelled with a cylinder (length and thickness) and the cylinder is correlated with the segmented protein map. Since the best solution is achieved by exhaustively searching in translation space (3D) and orientation space (2D), this method is computationally expensive. A related exhaustive search approach, designed for beta sheet detection uses a disk (planar) model for beta sheets.

